



Delft University of Technology

New LAMBDA toolbox for mixed-integer models estimation and evaluation

Massarweh, Lotfi; Verhagen, Sandra; Teunissen, Peter J.G.

DOI

[10.1007/s10291-024-01738-z](https://doi.org/10.1007/s10291-024-01738-z)

Publication date

2024

Document Version

Final published version

Published in

GPS Solutions

Citation (APA)

Massarweh, L., Verhagen, S., & Teunissen, P. J. G. (2024). New LAMBDA toolbox for mixed-integer models: estimation and evaluation. *GPS Solutions*, 29(1), Article 14. <https://doi.org/10.1007/s10291-024-01738-z>

Important note

To cite this publication, please use the final published version (if applicable).
Please check the document version above.

Copyright

Other than for strictly personal use, it is not permitted to download, forward or distribute the text or part of it, without the consent of the author(s) and/or copyright holder(s), unless the work is under an open content license such as Creative Commons.

Takedown policy

Please contact us and provide details if you believe this document breaches copyrights.
We will remove access to the work immediately and investigate your claim.



New LAMBDA toolbox for mixed-integer models: estimation and evaluation

Lotfi Massarweh¹ · Sandra Verhagen¹ · Peter J. G. Teunissen^{1,2,3}

Received: 25 June 2024 / Accepted: 23 August 2024
© The Author(s) 2024

Abstract

In this work we introduce the LAMBDA 4.0 toolbox, which provides an enhanced implementation for integer estimation, validation, and success rate evaluation. This free and open-source toolbox is a major update to LAMBDA 3.0 (2012), while it also integrates the functionalities from Ps-LAMBDA 1.0 (2013), thus respectively merging both *estimation* and *evaluation* capabilities. The new implementation provides redefined algorithms, such as an improved integer search strategy with a one-order reduction in the computational time, along with additional estimators: Vectorial Integer Bootstrapping (VIB), Integer Aperture Bootstrapping (IAB) and Best Integer Equivariant (BIE). This toolbox aims to become a valuable resource for researchers and/or practitioners dealing with mixed-integer models in high dimensions, e.g., terrestrial-based carrier-phase systems, multi-constellation Global Navigation Satellite Systems (GNSS), or other interferometric applications.

Keywords Least-squares AMBIGUITY Decorrelation Adjustment (LAMBDA) · Success Rate (SR) · Integer estimator · Integer Aperture estimator · Integer Equivariant estimator · Global Navigation Satellite System (GNSS)

Introduction

The Least-squares AMBIGUITY Decorrelation Adjustment (LAMBDA) method was introduced in Teunissen (1993) as a numerically efficient and statistically optimal solution approach to Integer Ambiguity Resolution (IAR) problems. Such problems arise in many GNSS and non-GNSS mixed-integer model applications (see Table 1). For GNSS mixed-integer models, the millimeter-level precision of the ambiguous carrier-phase measurements can be exploited

once the integer ambiguities are correctly resolved with high probability, also known as Success Rate (SR).

In this contribution we present the LAMBDA 4.0 toolbox, a new implementation dedicated to integer estimation, integer validation and SR computations. This new toolbox integrates all functionalities from LAMBDA 3.0 (Verhagen et al. 2012), and Ps-LAMBDA 1.0 (Verhagen et al. 2013), while incorporating newly redesigned algorithms that enhance the computational performance for high-dimensional problems. The novelties are not limited to computational aspects, since additional (classes of) estimators are implemented, including the Vectorial Integer Bootstrapping (Teunissen et al. 2021), Integer Aperture Bootstrapping (Teunissen 2005) and Best Integer Equivariant (Teunissen 2003a) solutions. In this way, we provide users with a larger collection of tools in support to several applications.

In Sect. 2, we discuss mixed-integer models, including three different classes of estimators. In Sect. 3, LAMBDA 4.0 is presented, where LAMBDA and Ps-LAMBDA capabilities are discussed, along with the software package provided to the user. In Sect. 4, we focus on ‘estimation’ and ‘evaluation’ capabilities for the new toolbox, providing some illustrative numerical examples. In Sect. 5, the main conclusions are summarized. A more detailed mathematical

The GPS Toolbox is a topical collection dedicated to highlighting algorithms and source code utilized by GNSS engineers and scientists. If you have a program or software package you would like to share with our readers, please submit a paper to the GPS Toolbox.

✉ Lotfi Massarweh
L.Massarweh@tudelft.nl

¹ Geoscience and Remote Sensing, Delft University of Technology, Delft, Netherlands

² Department of Infrastructure Engineering, The University of Melbourne, Melbourne, Australia

³ GNSS Research Centre, Curtin University, Perth, Australia

Table 1 Examples of applications dealing with IAR problems

	Application	Reference
GNSS	precise point positioning	(Teunissen 2020)
	integer cycle-slip resolution	(Teunissen and de Bakker 2015)
	time and frequency transfer	(Mi et al. 2023)
	atmosphere remote sensing	(Lu et al. 2018)
	carrier-phase attitude determination	(Giorgi 2011)
	relative navigation for S/C formation flying	(Buist 2013)
Non-GNSS	detection in MIMO communication systems	(Damen et al. 2003)
	InSAR permanent scatterer technique	(Kampes and Hanssen 2004)
	phase data for InSAR deformation monitoring	(Teunissen 2006)
	use of acoustic waves for underwater navigation	(Viegas and Cunha 2007)
	fringe phase observations from VLBI	(Hobiger et al. 2009)

documentation, hereinafter referred to as ‘LAMBDA Documentation’, is given as supplementary information to this publication.

Mixed-integer models

We start with a linear(ized) mixed-integer model, given $y \in \mathbb{R}^m$ as the vector of observables, and $Q_{yy} \in \mathbb{R}^{m \times m}$ its variance-covariance (vc-)matrix, such that

$$E\{y\} = Aa + Bb, \quad D\{y\} = Q_{yy} \quad (1)$$

where $E\{\cdot\}$ and $D\{\cdot\}$ are the expectation and dispersion operators, respectively. The vectors $a \in \mathbb{Z}^n$ and $b \in \mathbb{R}^p$ refer respectively to the integer ambiguities and real-valued parameters, while the full-rank design matrix is given by $[A, B] \in \mathbb{R}^{m \times (n+p)}$.

Usually, a three-step procedure is employed to solve such mixed-integer models, based on a weighted least-squares criterion, so considering the quadratic objective function

$$\|y - Aa - Bb\|_{Q_{yy}}^2 = \|\hat{e}\|_{Q_{yy}}^2 + \|\hat{a} - a\|_{Q_{\hat{a}\hat{a}}}^2 + \|\hat{b}(a) - b\|_{Q_{\hat{b}(a)\hat{b}(a)}}^2 \quad (2)$$

where $\|x\|_Q^2 = x^T Q^{-1} x$, while $\hat{e} = y - A\hat{a} - B\hat{b}$ refers to the least-squares residuals’ vector.

Following this orthogonal decomposition (Teunissen 1993), we compute

1. **Float solution**, where the integer constraints on the ambiguities are neglected, and a least-squares solution

is found assuming $a \in \mathbb{R}^n$ and $b \in \mathbb{R}^p$, thus providing the float estimators $\hat{a} \in \mathbb{R}^n$ and $\hat{b} \in \mathbb{R}^p$.

2. **Ambiguity resolution**, where starting with the ambiguity float estimator $\hat{a} \in \mathbb{R}^n$ and its vc-matrix $Q_{\hat{a}\hat{a}} \in \mathbb{R}^{n \times n}$, we obtain the fixed ambiguity estimator $\tilde{a} = \mathcal{J}_a(\hat{a})$ given a certain mapping function \mathcal{J}_a defined for the selected estimator.
3. **Fixed solution**, where the real-valued (*float*) parameter $\hat{b} \in \mathbb{R}^p$ are now conditionally updated onto the (*fixed*) ambiguities, so leading to the fixed solution $\tilde{a} = \hat{b}(\tilde{a})$, while we assume no additional constraints exist onto the \hat{b} -parameters.

The LAMBDA method (Teunissen 1995) exploits the ambiguity re-parametrization by an admissible transformation matrix $Z \in \mathbb{Z}^{n \times n}$, where $\hat{z} = Z^T \hat{a}$ with $\hat{z} \in \mathbb{R}^n$, which serves to decorrelate the ambiguity components. This Z -transformation process increases SR for some estimators, while the SR is invariant for the Integer Least-Squares (ILS) estimator, whereas its computational performance can substantially be enhanced.

Different classes of estimators

In Teunissen (2003c), three classes of estimators are introduced:

- I. **Integer estimators**, i.e. I-class;
- II. **Integer Aperture estimators**, i.e. IA-class;
- III. **Integer Equivariant estimators**, i.e. IE-class;

with a set relationship $I \subset IA \subset IE$, as shown in Fig. 1 with one example per class.

Each class is characterized by different properties based on the family of maps \mathcal{J}_a being defined. The I-class (Teunissen 1999) is the most restrictive class, with many-to-one mapping functions defining *pull-in regions* that leave no gaps, have no overlaps and are invariant to integer translations. The IA-class (Teunissen 2003b) is defined by dropping the ‘no gaps’ condition, and so-called *aperture regions* can be defined. The IE-class (Teunissen 2002) is the largest class, where the ‘no overlaps’ condition is relaxed, while the ‘integer remove-restore’ property is still satisfied. We refer to Verhagen (2005) and the ‘LAMBDA Documentation’ for more mathematical details.

LAMBDA 4.0 description

The new toolbox merges functionalities from LAMBDA 3.0 (Verhagen et al. 2012) and Ps-LAMBDA 1.0 (Verhagen et al. 2013), while providing advanced algorithms and

Fig. 1 Overview of the three main classes and their set relationship, including an example of estimator per each class: Integer Least-Squares (ILS), Integer Aperture Bootstrapping (IAB) and Best Integer Equivariant (BIE)

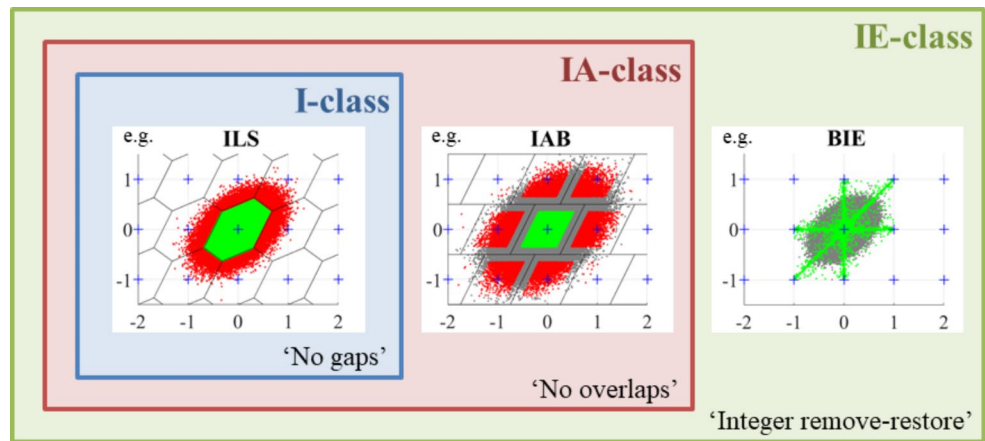
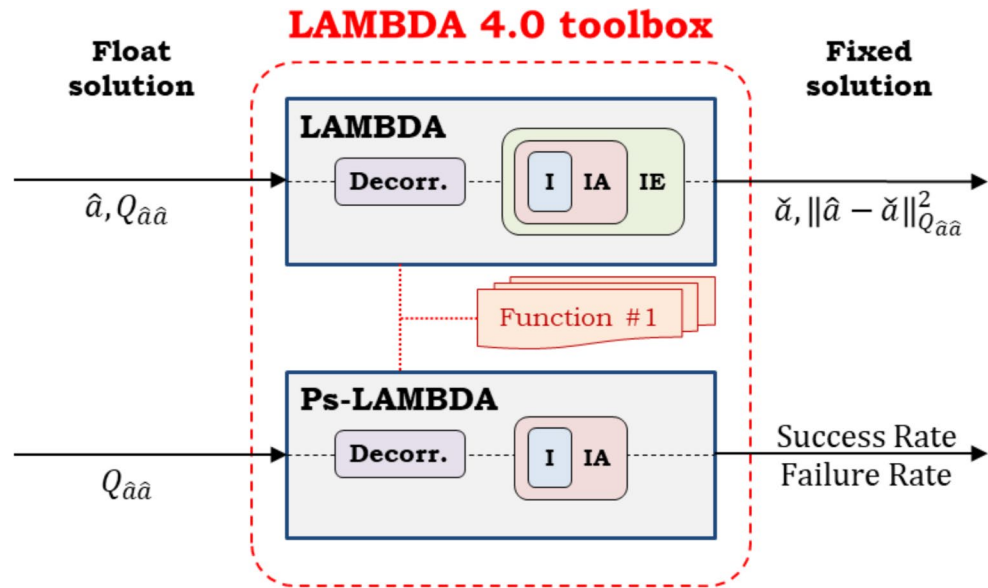


Fig. 2 Flowchart of the LAMBDA 4.0 toolbox



additional estimators. A flowchart is shown in Fig. 2, with both LAMBDA and Ps-LAMBDA routines, respectively adopted for ‘estimation’ and ‘evaluation’.

LAMBDA capabilities

The main LAMBDA script takes as inputs the \hat{a} -vector and $Q_{\hat{a}\hat{a}}$ -matrix, along with relevant configuration parameters. The decorrelation starts with an L^TDL -decomposition, followed by a Z -transformation given an admissible matrix $Z \in \mathbb{Z}^{n \times n}$ (unimodular), so $Q_{\hat{z}\hat{z}} = Z^T Q_{\hat{a}\hat{a}} Z$. This matrix Z also sorts ambiguities based on their conditional variances, so enabling the selection of a suitable subset of most precise components needed for Partial Ambiguity Resolution (PAR). An overview of LAMBDA-related methods is given in Fig. 3.

A new integer search strategy is adopted (Sect. 4.2.1), where a one-order reduction in computational time is possible, with large computational benefits for high-dimensional

problems. Moreover, new coefficients (Hou et al. 2016) are adopted for the critical value of the Fixed Failure-rate Ratio Test (FFRT) solution, based on fitting functions. Lastly, new estimators are introduced:

- **I-class:** VIB (Teunissen et al. 2021), based on IR or ILS estimators, while supporting any arbitrary block partitioning of the whole ambiguity set;
- **IA-class:** IAB (Teunissen 2005), for a user-defined aperture parameter $\beta_{\text{IAB}} \in (0, 1]$ or a maximum bootstrapping failure rate selected by the user;
- **IE-class:** BIE (Teunissen 2003a), approximated here by a finite summation within a search ellipsoid for a user-defined significance level $\alpha_{\text{BIE}} \ll 1$.

Fig. 3 The LAMBDA functions implemented in LAMBDA 4.0 toolbox are listed, including their class, a short description and some relevant configuration options

LAMBDA	Class	Description	Options
estimatorIR	I	Integer Rounding	-
estimatorIB	I	Integer Bootstrapping	-
estimatorILS	I	Integer Least Squares (search-and-shrink)	• # of candidates
estimatorILS_enum	I	Integer Least Squares (enumeration)	• # of candidates
estimatorPAR	I	Partial Ambiguity Resolution (with ILS estimator)	• # of candidates • Minimum SR
estimatorVIB	I	Vectorial Integer Bootstrapping (with IR or ILS estimator)	• Use IR or ILS • Partitioning of blocks
estimatorIA_RT	IA	Integer Aperture w/ Ratio Test	• Aperture parameter μ_{RT} • Maximum FR
estimatorIAB	IA	Integer Aperture Bootstrapping	• Aperture parameter β_{IAB} • Maximum FR
estimatorBIE	IE	Best Integer Equivariant (finite approximation)	• Significance level α_{BIE}

Fig. 4 The Ps-LAMBDA functions implemented in LAMBDA 4.0 toolbox are listed here, including a short description and their relation to popular Integer estimators

Ps-LAMBDA	Description	IR	VIB-IR	IB	VIB-ILS	ILS
IBexact	Integer Bootstrapping (exact SR, analytical)	UB	UB	exact	LB	LB
ADOPapprox	ADOP method (approximation)	UB	UB	UB	approx.	approx.
LB_Variance	Variance method (Lower Bound)	LB	LB	LB	LB	LB
UB_ADOP	ADOP method (Upper Bound)	UB	UB	UB	UB	UB
LB_Eigenvalue	Eigenvalue method (Lower Bound)	-	-	-	-	LB
UB_Eigenvalue	Eigenvalue method (Upper Bound)	UB	UB	UB	UB	UB
LB_Pullin	Pull-in region method (Lower Bound)	-	-	-	-	LB
UB_Pullin	Pull-in region method (Upper Bound)	UB	UB	UB	UB	UB
Numerical	Numerical (simulation-based)	approx.	approx.	approx.	approx.	approx.

Ps-LAMBDA capabilities

The main Ps-LAMBDA script takes as input only the $Q_{\hat{a}\hat{a}}$ matrix, along with a flag to enable the decorrelation of ambiguities, so users can still check the impact of different decorrelation strategies on each SR bound/approximation. The overview of Ps-LAMBDA-related methods is given in Fig. 4, while we refer to Verhagen et al. (2013) for more details.

The different methods serve as lower/upper bounds (LB/UB), or even approximation for the SR, while we recall the performance ordering (Teunissen et al. 2021):

$$IR \leq VIB_{IR} \leq IB \leq VIB_{ILS} \leq ILS \quad (3)$$

with Integer Rounding (IR) and Integer Least-Squares (ILS), which might also be applied vectorially as VIB_{IR} and VIB_{ILS} estimators, respectively. An exact SR can be computed only

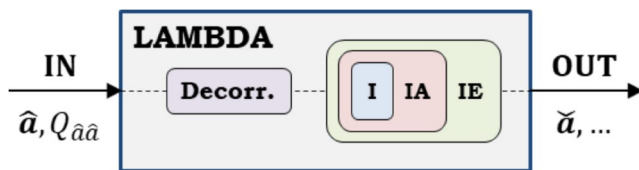
for Integer Bootstrapping (IB), while numerical simulations are available as approximation for all I- or IA-estimators of this toolbox, and Ps-LAMBDA performance can benefit from the enhanced algorithms implemented here.

Software package

The LAMBDA 4.0 software package contains different files/folders (see Table 2). Both ‘LAMBDA’ and ‘Ps_LAMBDA’ main scripts make use of the functionalities included in a dedicated “LAMBDA_toolbox” folder. However, more advanced users might benefit from directly using these functions in their software without the need to follow the logic defined by these main scripts. These can still easily be included into existing software applications, e.g., as for LAMBDA legacy versions already integrated in the “raPP-Pid” software package (Glaner and Weber 2023).

Table 2 List of the principal files and/or folders in this software package

File/Folder	Description
README.txt	Text file with content overview
LAMBDA	Main script with LAMBDA functionalities
Ps_LAMBDA	Main script with Ps-LAMBDA functionalities
\LAMBDA_toolbox	Folder with all toolbox functionalities
\LAMBDA_examples	Folder with some illustrative examples
\LAMBDA_papers	Folder with some relevant publications
LAMBDA – Documentation.pdf	PDF with main mathematical descriptions
LAMBDA – User Manual.pdf	PDF with the toolbox guide (per environment)

**Fig. 5** LAMBDA main script supporting different classes of estimators

A detailed description of these new functionalities can be found in the supplementary material (see ‘LAMBDA Documentation’). The current MATLAB implementation is based on v2024a, and it does not require any additional toolboxes. Moreover, this has been tested for backward compatibility starting with version 2018b, while a Python 3 version, including its dedicated user manual, is currently under development.

LAMBDA 4.0: estimation and evaluation

Estimation in the I-class, IA-class and IE-class

This LAMBDA 4.0 implementation offers a versatile toolbox with several estimators suitable for different problems,

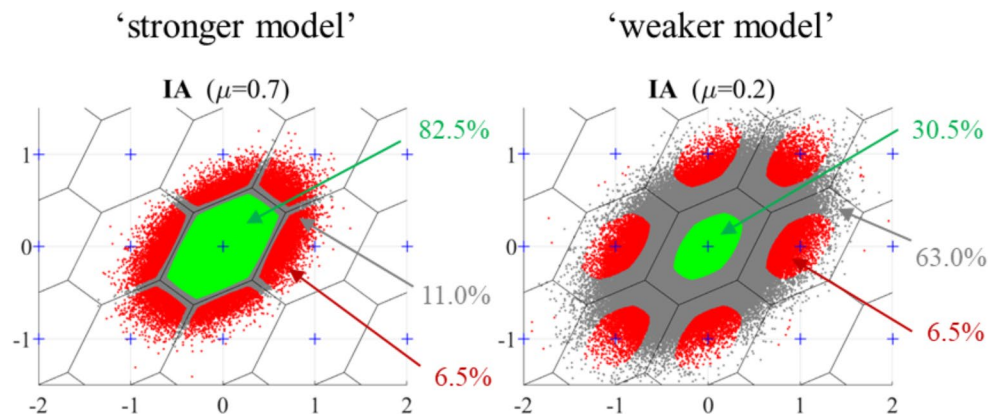
where users have access to three classes of estimators (see Fig. 5).

In some applications, it is important that users have control over the failure rate, and two different solutions could achieve this: a model-driven I-estimator and a data-driven IA-estimator. The former one uses PAR, where only part of the ambiguity vector is estimated, whereas the latter considers part of the pull-in region for the integer mapping. Figure 6 shows a graphical example of IA-estimator based on ratio test, where a stronger and a weaker model are considered respectively in the left and right plots. The selection of the aperture parameter μ is fundamental for correctly ‘controlling’ the failure rate, where different aperture values are adopted for the two models, while still having a similar failure rate.

Another example concerns vectorial IB solutions, more suitable for high-dimensional problems. A VIB-based method is currently implemented in GROOPS software (Mayer-Gürr et al. 2021), where it is possible to resolve thousands of ambiguity components within a few tenths of a second in the context of small global networks for Orbit Determination and Time Synchronization (ODTS), see Massarweh et al. (2021).

Within the IE-class, the BIE solution is optimal in the minimum Mean Squared Error (MSE) sense. This property is beneficial for precise positioning applications, as shown by Odolinski and Teunissen (2020) in the context of multi-GNSS Real-Time Kinematics (RTK) using low-cost receivers, as well as by Yang et al. (2024) for PPP-AR applications. These BIE solutions will always outperform – in the MSE sense – both float and fixed solutions.

A numerical simulation is shown in Fig. 7, based on GPS (L1-only) single-baseline relative (kinematic) positioning with 6 satellites tracked (at 30s). In this illustrative example, we neglect the atmospheric delays (e.g., short baseline) and we adopt an elevation weighting $\propto 1/\sin(\text{el})$, while having 30 cm and 3 mm standard deviation for the undifferenced code and phase observations (at zenith). Using 100,000 simulations, we compute the MSE ratio of different ‘fixed’

Fig. 6 A comparison between a stronger and a weaker model is given using two different ratio tests, respectively for $\mu = 0.7$ and $\mu = 0.2$. Three regions can be observed, related to values of Success Rate (green), Failure Rate (red) and Undecided Rate (grey)

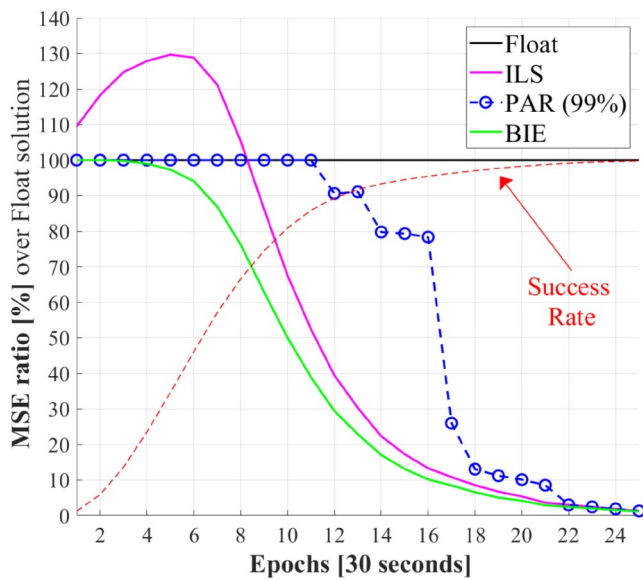


Fig. 7 The ratio [%] of MSE of the baseline positioning coordinates with respect to the float solution is shown for different estimators based on GPS single-baseline single-frequency kinematic positioning, while using 30 cm/3 mm standard deviation for the undifferenced code/phase observations

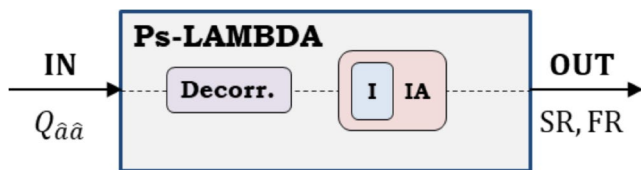
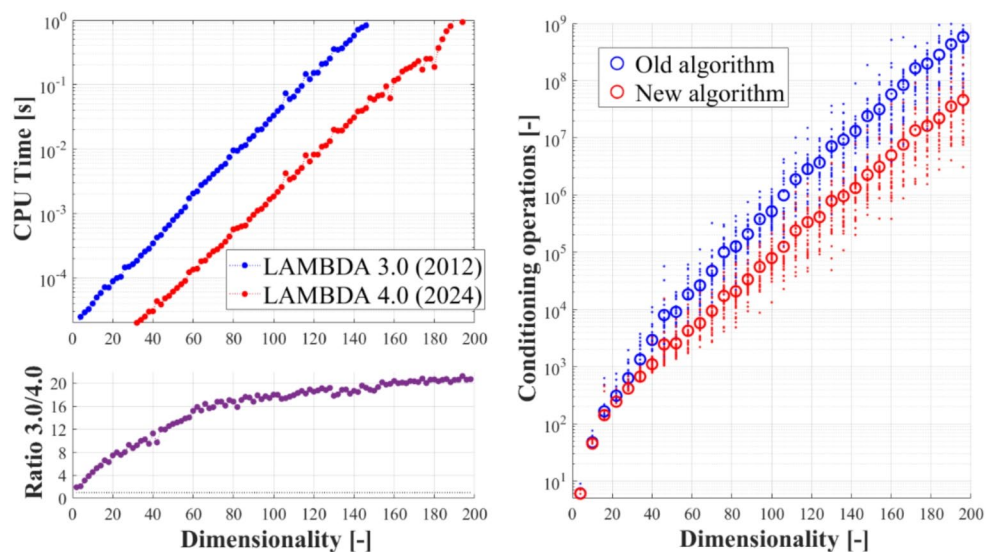


Fig. 8 Ps-LAMBDA main script supporting different classes of estimators

solutions with respect to the ‘float’ solution. A PAR solution is also shown in Fig. 7, based on an SR > 99.0% criterion, where only a subset of the ambiguities can be fixed, and improvements compared to the ‘float’ are negligible during

Fig. 9 A numerical comparison is shown between LAMBDA 3.0 (OLD) and LAMBDA 4.0 (NEW) algorithm in terms of search computations for the optimal ILS solution



the first epochs. At low SR values, the ILS estimator – optimal in terms of SR – might also lead to worse-than-float performance, whereas the BIE estimator is capable of outperforming all these solutions and it provides a minimum MSE value for the positioning coordinates computed here. We refer to Brack et al. (2023) for additional BIE-related results.

Numerical and statistical evaluations

For experimental and designing purposes, it is important to compute the relevant statistical measure of the different estimators, e.g. SR for the I-class, or also FR for the IA-class, as enabled in an efficient way by the new toolbox (see Fig. 8).

Numerical evaluations

In terms of numerical performance, the integer search strategy introduced by Ghasemmehdi and Agrell (2011) has been adopted, which is beneficial for both estimation and evaluation functionalities. The main advantage of this new search strategy is the removal of non-necessary conditioning operations when spanning (down) the search tree, see (ibid.). An example is provided in Fig. 9, considering the old (in blue) and new (in red) search algorithms; see also Jazaeri et al. (2014).

The numerical test in Fig. 9 is based on a single-baseline geometry-free ionosphere-fixed model using L1 + L2 signals, with a standard deviation of 20 cm/2 mm respectively for the undifferenced code/phase observations. The number of satellites varies between 2 and 100 to increase the problem dimensionality, with larger improvements expected at higher dimensionalities. The computational time is shown averaged over 1000 runs (top-left plot), along with the ratio between LAMBDA 3.0 and 4.0 (bottom-left

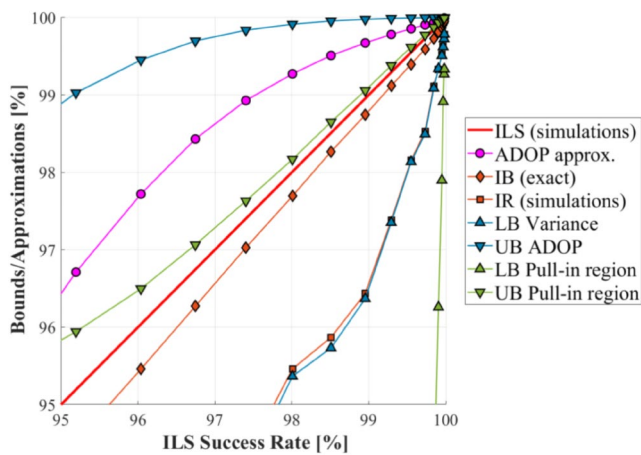


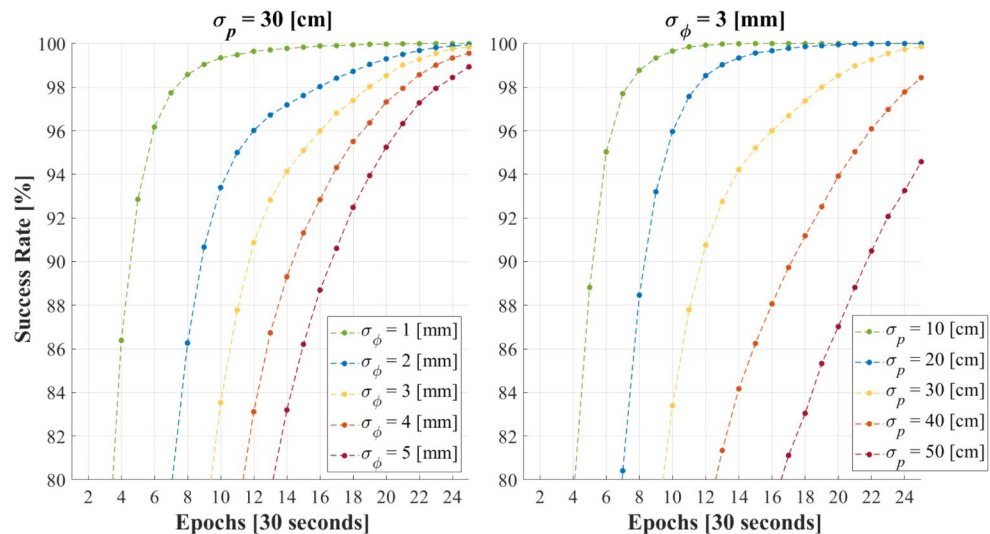
Fig. 10 A few different bounds or approximations are compared with respect to the SR of ILS taken here as reference (in the range 95–100%), based on the example from Fig. 7, while IR and ILS numerical simulations are computed using 10^6 samples

plot). Moreover, the number of conditioning operations is illustrated (right plot), showing the results for each single run (dots), based on different float samples, along with their averages (circles). This new strategy does not only enhance I-estimators, such as ILS¹, PAR and VIB-ILS, but it has a positive impact also on Ps-LAMBDA functionalities, e.g., for SR/FR simulations.

Statistical evaluations

In Fig. 10, we compare a few different SR bounds and approximations with respect to the ILS one, which has been numerically computed for the problem adopted in Fig. 7. In this example, the pull-in region method (in green) provides

Fig. 11 The SR of ILS is computed using 10^6 samples, based on the example of Fig. 7, where standard deviation for the undifferenced phase σ_ϕ (left plot) and code σ_p (right plot) observations has been varied. An elevation weighting scheme is adopted in all simulations



¹ This 2011-algorithm has also been adopted in the MLAMBDA implementation starting from its 2016 version <https://www.cs.mcgill.ca/~chang/software/>, but limited only to the ILS estimator.

a close upper bound to ILS estimator (red line) for high SR values, while the variance method (in blue) is a close lower bound to IR estimator (orange square symbol). See Wang et al. (2016) for additional examples.

Moreover, two important cases could be considered (Teunissen 2000):

- 1) SR sensitivity for changes in the stochastic model of observations.
- 2) SR sensitivity when using an incorrect stochastic model of observations.

In the first case, this analysis allows users to calculate how a precision improvement of their data would affect the SR. In the second case, it provides users with a way to understand how accurate they would need to know their observables' variance-covariance matrix to maintain quasi-optimal performance in the ambiguity fixing. Hence, this provides a diagnostics to assess the impact on SR due to stochastic misspecifications.

We start with the first case, where we consider in Fig. 11 the model adopted in Fig. 7, and we vary the standard deviation for the undifferenced phase (left plot) or code (right plot) observations. Then, we compute the SR of ILS based on 10^6 samples, and we focus on the range 80-to-100%. A similar sensitivity analysis can be performed with other I- and IA-estimators, as well as considering bounds and/or approximations. See Nardo et al. (2016) for additional examples.

For the second case, we present an example on the adoption of an incorrect stochastic model, which can negatively affect IAR performance. We consider a (short) single-base-line GPS (L1+L2) model, with 7 satellites tracked on a single epoch, having 30 cm/3 mm for the standard deviation

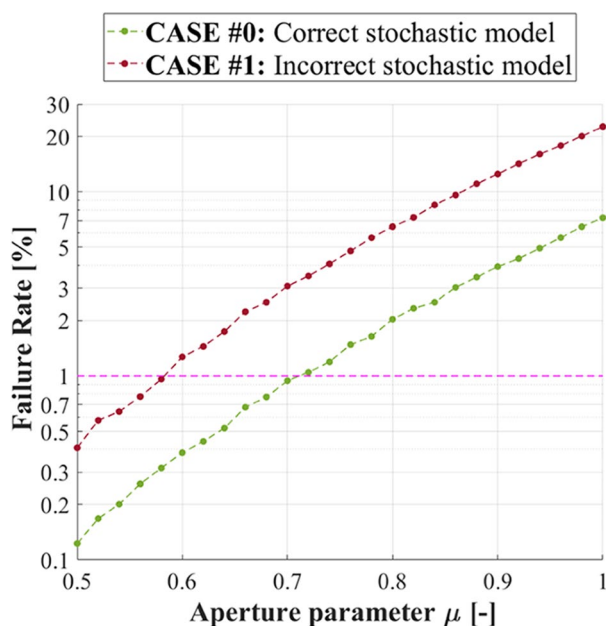


Fig. 12 The failure rate is numerically computed for a (short) single-baseline GPS (L1 + L2) model based on an Integer Aperture estimator with Ratio Test, where different values of the aperture parameter μ are used. An arbitrary user-defined threshold (FR < 1%) is shown in magenta

of undifferenced code/phase data, respectively. The correct stochastic model is based on an elevation weighting scheme $\propto 1/\sin(\text{el})$, while for the float solution computation we consider an incorrect stochastic model without any elevation weighting. The Ps-LAMBDA functionalities enable users to compare the correct and incorrect stochastic models, so numerically computing the failure rate for an IA-estimator, e.g., with Ratio Test, while varying its aperture parameter $\mu \leq 1$.

The results are shown in Fig. 12, where SR of ILS is 92.9% or 77.3% when a correct or an incorrect model is used, respectively. Given different μ -values between 0.5 and 1.0, we can compute the FR, with a user-defined threshold (magenta dashed line) set here to 1%. Given $\mu = 0.7$, e.g., the FR is 0.9% or 3.0%, and the maximum FR threshold condition will be fulfilled only with the correct stochastic model.

Conclusions

In this contribution we introduce the LAMBDA 4.0 toolbox, a new implementation for the integer estimation, integer validation and success rate computation. This new toolbox builds its foundations over two legacy software implementations: LAMBDA 3.0 and Ps-LAMBDA 1.0, respectively introduced by Verhagen et al. (2012) and by Verhagen et

al. (2013). Several modular functionalities are provided and they can be used standalone to be easily integrated into existing GNSS or non-GNSS processing software.

The LAMBDA 4.0 toolbox enhances the computational performances based on new routines to tackle any mixed-integer problem. For instance, an improved search strategy for optimal Integer Least-Squares (ILS) solutions has been implemented and becomes beneficial in many other Ps-LAMBDA functionalities. Moreover, new (classes of) estimators have been introduced, e.g., a flexible Vectorial Integer Bootstrapping (VIB) formulation for the high-dimensional problems, an Integer Aperture Bootstrapping (IAB) solution for the controlled failure rate applications, an optimal BIE solution that always outperforms – in the minimum Mean Squared Error sense – both float and fixed solutions.

The newly developed toolbox comes in response to the current need for advanced solutions to tackle high-dimensional problems in both an efficient and reliable way. Hence, this LAMBDA 4.0 toolbox can support many applications, e.g. for multi-GNSS and multi-frequency mixed-integer models arising in PPP-RTK network estimation (Teunissen and Khodabandeh 2015), frequency-varying carrier phase signals (Khodabandeh and Teunissen 2023) and in view to the future deployment of large satellite constellations in low-Earth orbit (LEO) tracked on ground. This landscape of possibilities is not limited to GNSS applications but it is expected to benefit all researchers dealing with mixed-integer models, thus providing a simple, versatile and effective tool to the research community.

Supplementary Information The online version contains supplementary material available at <https://doi.org/10.1007/s10291-024-01738-z>.

Acknowledgements The authors would like to thank the software reviewers who have evaluated and tested the toolbox in its early beta version: Kan Wang (NTSC Chinese Academy of Sciences), Bofeng Li and his research team (Tongji University), Safoora Zaminpardaz (RMIT University), Amir Khodabandeh (University of Melbourne), Daniel Medina (German Aerospace Center, DLR) and Francesco Darugna (Geo++ GmbH).

Author contributions L.M. developed the software based on previous implementations. All the authors contributed equally to the LAMBDA 4.0 toolbox conceptualization and to this manuscript realization.

Data availability All the data and supporting material is made available in the LAMBDA Software Package that can directly be downloaded at <http://pntlab.tudelft.nl/LAMBDA>, or it can be requested directly from the LAMBDA Team (LAMBDAtoolbox-CITG-GRS@tudelft.nl).

Declarations

Competing interests The authors declare no competing interests.

Open Access This article is licensed under a Creative Commons Attribution 4.0 International License, which permits use, sharing, adaptation, distribution and reproduction in any medium or format, as long as you give appropriate credit to the original author(s) and the source, provide a link to the Creative Commons licence, and indicate if changes were made. The images or other third party material in this article are included in the article's Creative Commons licence, unless indicated otherwise in a credit line to the material. If material is not included in the article's Creative Commons licence and your intended use is not permitted by statutory regulation or exceeds the permitted use, you will need to obtain permission directly from the copyright holder. To view a copy of this licence, visit <http://creativecommons.org/licenses/by/4.0/>.

References

- Brack A, Männel B, Schuh H (2023) Two-epoch centimeter-level PPP-RTK without external atmospheric corrections using best integer-equivariant estimation. *GPS Solut* 27:12
- Buist PJ (2013) Multi-platform Integrated Positioning and Attitude Determination using GNSS. Ph.D. dissertation, Delft University of Technology, Delft, The Netherlands
- Damen MO, El Gamal H, Caire G (2003) On maximum-likelihood detection and the search for the closest lattice point. In *IEEE Transactions on Information Theory*, vol. 49, no. 10, pp. 2389–2402, Oct. 2003
- Ghasemmehdi A, Agrell E (2011) Faster Recursions in Sphere Decoding. In *IEEE Transactions on Information Theory*, vol. 57, no. 6, pp. 3530–3536, June 2011
- Giorgi G (2011) GNSS Carrier Phase-Based Attitude Determination: Estimation and Applications. Ph.D. dissertation, Delft University of Technology, Delft, The Netherlands
- Glaner MF, Weber R (2023) An open-source software package for Precise Point Positioning: raPPPid. *GPS Solut* 27:174
- Hobiger T, Sekido M, Koyama Y, Kondo T (2009) Integer phase ambiguity estimation in next-generation geodetic very long baseline interferometry. *Adv Space Res* 43(1):187–192
- Hou Y, Verhagen S, Wu J (2016) An Efficient Implementation of Fixed Failure-Rate Ratio Test for GNSS Ambiguity Resolution. *Sensors*. 2016; 16(7):945
- Jazaeri S, Amiri-Simkooei A, Sharifi M (2014) Modified weighted integer least squares estimations for GNSS IAR. *Surv Rev* 46(335):112–121
- Kampes BM, Hanssen RF (2004) Ambiguity resolution for permanent scatterer interferometry, in *IEEE Transactions on Geoscience and Remote Sensing*, vol. 42, no. 11, pp. 2446–2453, Nov. 2004
- Khodabandeh A, Teunissen PJG (2023) Ambiguity-Fixing in Frequency-Varying Carrier Phase Measurements: Global Navigation Satellite System and Terrestrial Examples. *NAVIGATION: Journal of the Institute of Navigation*, 70(2)
- Lu C, Li X, Cheng J, Dick G, Ge M, Wickert J, Schuh H (2018) Real-Time Tropospheric Delay Retrieval from Multi-GNSS PPP Ambiguity Resolution: Validation with Final Troposphere Products and a Numerical Weather Model. *Remote Sensing*. 2018; 10(3):481
- Massarweh L, Strasser S, Mayer-Gürr T (2021) On vectorial integer bootstrapping implementations in the estimation of satellite orbits and clocks based on small global networks. *Adv Space Res* 68(11):4303–4320
- Mayer-Gürr T, Behzadpour S, Eicker A, Ellmer M, Koch B, Krauss S, Pock C, Rieser D, Strasser S, Süßner-Rechberger B et al (2021) GROOPS: a software toolkit for gravity field recovery and GNSS processing. *Comput Geosci* 155(104):864
- Mi X, Zhang B, El-Mowafy A et al (2023) Undifferenced and uncombined GNSS time and frequency transfer with integer ambiguity resolution. *J Geod* 97:13
- Nardo A, Li B, Teunissen PJG (2016) Partial ambiguity resolution for ground and space-based applications in a GPS + Galileo scenario: a simulation study. *Adv Space Res* 57(1):30–45
- Odolinski R, Teunissen PJG (2020) Best integer equivariant estimation: performance analysis using real data collected by low-cost, single- and dual-frequency, multi-GNSS receivers for short- to long-baseline RTK positioning. *J Geod* 94:91
- Teunissen PJG (1993) Least-squares estimation of the integer GPS ambiguities. In *IAG General Meeting. Invited lecture. Section IV Theory and Methodology*
- Teunissen PJG (1995) The least-squares ambiguity decorrelation adjustment: a method for fast GPS integer ambiguity estimation. *J Geod* 70(1):65–82
- Teunissen PJG (1999) The probability distribution of the GPS baseline for a class of integer ambiguity estimators. *J Geodesy* 73:275–284
- Teunissen PJG (2000) The success rate and precision of GPS ambiguities. *J Geodesy* 74:321–326
- Teunissen PJG (2002) A new class of GNSS ambiguity estimators. *Artif Satellites* 37(4):111–120
- Teunissen PJG (2003a) Theory of integer equivariant estimation with application to GNSS. *J Geodesy* 77:402–410
- Teunissen PJG (2003b) Integer aperture GNSS ambiguity resolution. *Artif Satellites* 38(3):79–88
- Teunissen PJG (2003c) Towards a unified theory of GNSS ambiguity resolution. *J Global Position Syst* 2(1):1–12
- Teunissen PJG (2005) Integer aperture bootstrapping: a new GNSS ambiguity estimator with controllable fail-rate. *J Geodesy* 79:389–397
- Teunissen PJG (2006) On InSAR ambiguity resolution for deformation monitoring. *Artif Satellites* 41(1):19–22
- Teunissen PJG (2020) GNSS precise point positioning. In: *Position, Navigation, and Timing Technologies in the 21st Century: integrated satellite navigation, sensor systems, and civil applications*, vol 1, pp 503–528
- Teunissen PJG, de Bakker PF (2015) Multivariate Integer Cycle-Slip Resolution: A Single-Channel Analysis. In: Sneeuw, N., Novák, P., Crespi, M., Sansò, F. (eds) *VIII Hotine-Marussi Symposium on Mathematical Geodesy*. International Association of Geodesy Symposia, vol 142. Springer, Cham
- Teunissen PJG, Khodabandeh A (2015) Review and principles of PPP-RTK methods. *J Geod* 89:217–240
- Teunissen PJG, Massarweh L, Verhagen S (2021) Vectorial integer bootstrapping: flexible integer estimation with application to GNSS. *J Geod* 95, 99 (2021)
- Verhagen S (2005) The GNSS integer ambiguities: Estimation and validation. Ph.D. dissertation, Delft University of Technology, Delft, The Netherlands
- Verhagen S, Li B, Teunissen PJG (2012) LAMBDA–Matlab implementation, version 3.0. Delft University of Technology and Curtin University
- Verhagen S, Li B, Teunissen PJG (2013) Ps-LAMBDA: ambiguity success rate evaluation Software for interferometric applications. *Comput Geosci* 54:361–376
- Viegas DCdN, Cunha SR (2007) Precise Positioning by Phase Processing of Sound Waves. In *IEEE Transactions on Signal Processing*, vol. 55, no. 12, pp. 5731–5738, Dec. 2007
- Wang L, Feng Y, Guo J, Wang C (2016) Impact of Decorrelation on Success Rate Bounds of Ambiguity Estimation. *J Navig* 69(5):1061–1081
- Yang Y, Zhou F, Song S (2024) Improving precise point positioning (PPP) performance with best integer equivariant (BIE) estimator. *GPS Solut* 28:50

Publisher's note Springer Nature remains neutral with regard to jurisdictional claims in published maps and institutional affiliations.